National Aeronautics and Space Administration

Orbital Debris Quarterly News

Volume 11, Issue 3

July 2007

Inside...

A publication of

The NASA Orbital Debris Program Office

UN Committee Accepts Space Debris Mitigation Guidelines

In February 2007 the Scientific and Technical Subcommittee (STSC) of the United Nations' Committee on the Peaceful Uses of Outer Space (COPUOS) completed a multi-year work plan with the adoption of a consensus set of space debris mitigation guidelines (Orbital Debris Quarterly News, 11-2, p.1). The full COPUOS, at its latest meeting in Vienna, Austria, during 6-15 June, has also accepted these guidelines.

COPUOS was established by the United Nations General Assembly in 1959 to review the scope of international cooperation in the peaceful uses of outer space, to devise programs in this field to be undertaken under the auspices of the United Nations, to encourage continued research and the dissemination of information on outer space matters, and to study legal problems arising from the exploration of outer space. The COPUOS now includes 67 Member States.

The STSC will continue to include space debris as an agenda item for its annual meetings. Beginning in 2008 Member States are encouraged to report their progress in implementing the new UN space debris mitigation guidelines. ♦

Detection of Debris from Chinese ASAT Test Increases; One Minor Fragmentation Event in Second Quarter of 2007

The extent of the debris cloud created by the destruction of the Fengyun-1C meteorological satellite on 11 January 2007 by a Chinese ballistic interceptor is becoming more apparent as routine and special radar observations of the fragments provide more data. By the end of June 2007 the U.S. Space Surveillance Network (SSN) was tracking more than 2200 objects with a size of at least 5 cm.

More than 1900 of these debris had been officially cataloged, making the event by far the worst satellite fragmentation of the space age. The Chinese anti-satellite (ASAT) test coupled with other satellite breakups in the first quarter of the year has resulted in an increase of fragmentation debris in Earth

continued on page 2

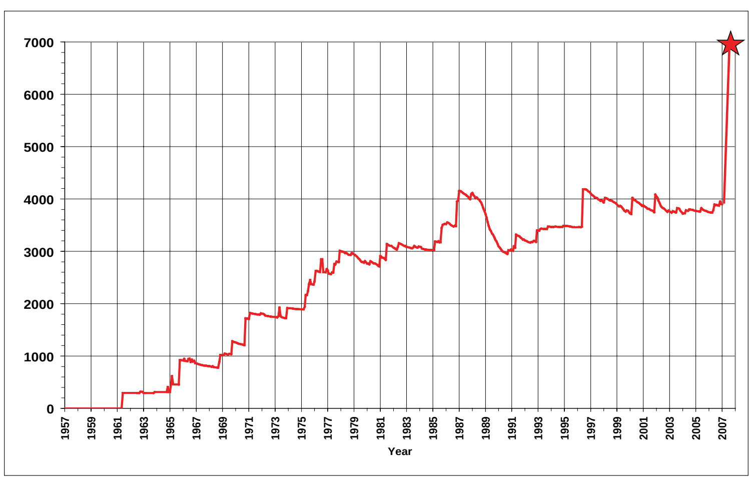

Figure 1. The total number of known fragmentation debris in Earth orbit increased by about 75% during the first quarter of 2007.

Detection of Debris

continued from page 1

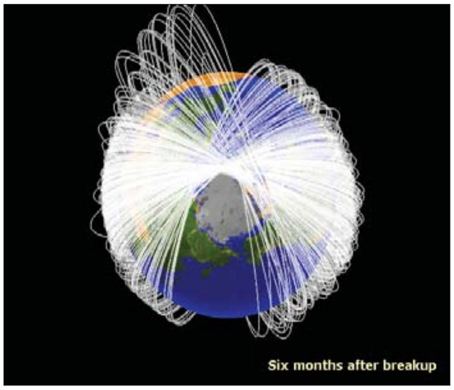

Figure 2. The debris cloud from the Fengyun-1C spacecraft is rapidly dispersing.

orbit of an estimated 75% (Figure 1).

The Fengyun-1C debris cloud extends from 200 km to 4000 km in altitude, with the highest concentration near the breakup altitude of approximately 850 km. The debris orbits are rapidly spreading (Figure 2) and will essentially encircle the globe by the end of the year. Only a few known debris had reentered more than five months after the test, and the majority will remain in orbit for many decades.

The large number of debris from Fengyun-1C are posing greater collision risks for spacecraft operating in low Earth orbit. The number of close approaches has risen significantly. On 22 June, NASA's Terra spacecraft had to execute a collision avoidance maneuver to evade a fragment from Fengyun-1C that was on a trajectory which would have passed within 19 meters of Terra.

After a flurry of satellite breakups in the first quarter of 2007, the next three months witnessed only one minor fragmentation classified as an anomalous event. An anomalous event is normally characterized by the release of only one or a few debris with very small separation velocities. The debris appear to "fall-off" their parent satellites, probably due to environmental degradation or small particle impacts (Johnson, 2004).

In April a new piece (U.S. Satellite Number 31408) from the derelict U.S. Seasat spacecraft (International Designator 1978-064A, U.S. Satellite Number 10967) was detected. This was the 15th debris from Seasat cataloged since 1983 and the fourth seen during the past four years (Figure 3). These debris exhibit a variety of ballistic coefficients, but all decay relatively rapidly compared to Seasat itself, which is in a stable, nearly circular orbit near 750 km. Additional debris have been briefly detected from Seasat, but they have reentered prior to being cataloged. The source of the debris could be either the spacecraft or the Agena upper stage to which it is still attached.

Early in 2006 an anomalous event involving the 46-year-old Vanguard 3 was detected (Orbital Debris Quarterly News, 10-3, p. 2). A second piece has now been cataloged (U.S. Satellite Number 31405), and it is likely to have also separated from Vanguard 3 in 2006, possibly about the time of the first piece. The newly discovered debris is decaying at a slower pace than the debris seen last year, but both are falling back to Earth much faster than Vanguard 3 from its orbit of 500 km by 3300 km.

1. Johnson, N.L., "Environmentally-Induced Debris Sources", *Advances in Space Research*, Vol. 34, Issue 5, pp. 993-999, 2004. ♦

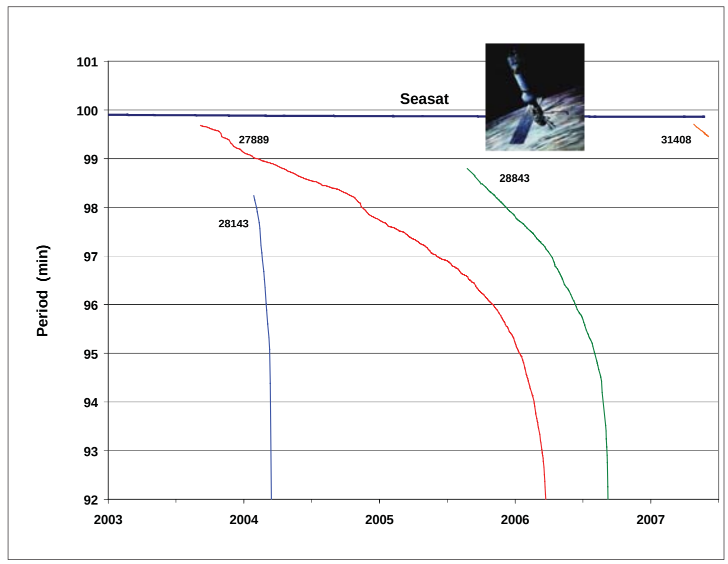

Figure 3. A new piece of debris separated from the Seasat spacecraft in early 2007.

PROJECT REVIEWS

Investigation of MMOD Impact on STS-115 Shuttle Payload Bay Door Radiator

J. HYDE, E. CHRISTIANSEN, D. LEAR, J. KERR, F. LYONS, J. YASENSKY

1. Introduction

The Orbiter radiator system consists of eight individual 4.6 m x 3.2 m panels with four located on the inside of each payload bay door. Forward panels #1 and #2 are 2.3 cm thick while the aft panels #3 and #4 have a smaller overall thickness of 1.3 cm. The honeycomb radiator panels consist of 0.028 cm thick Aluminum 2024-T81 facesheets and Al5056-H39 cores. The face-sheets are topped with 0.005 in. (0.127 mm) silver-Teflon tape. The inside of the Shuttle payload bay doors are closed during

continued on page 3

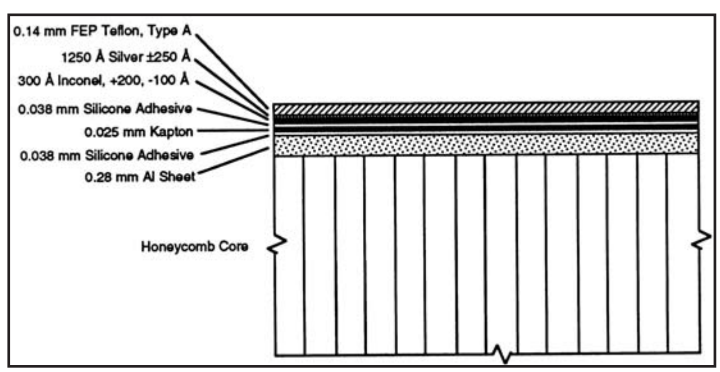

Figure 1. Cross section of orbiter radiator facesheet.

MMOD Impact

continued from page 2

ascent and reentry, limiting damage to the on-orbit portion of the mission.

2. Post Flight Inspection

Post-flight space inspections at the Kennedy Space Center (KSC) following the STS-115 mission revealed a large micro-meteoroid/orbital debris (MMOD) impact near the hinge line on the #4 starboard payload bay door radiator panel. The features of this impact make it the largest ever recorded on an orbiter payload bay door radiator. The general location of the damage site and the adjacent radiator panels can be seen in Figure 2. Initial measurements of the defect indicated that the hole in the facesheet was 0.108 in. (2.74 mm) in diameter. Figure 3 shows an image of the front side damage. Subsequent observations revealed exit damage on the rear facesheet. Impact damage features on the rear facesheet included a 0.03 in. diameter hole (0.76 mm), a ~0.05 in. tall bulge (~1.3 mm), and a larger ~0.2 in. tall bulge (~5.1 mm) that exhibited a crack over 0.27 in. (6.8 mm) long. A large ~1 in. (25 mm) diameter region of the honeycomb core was also damaged. Refer to Figure 4 for an image of the backside damage to the panel. No damage

continued on page 4

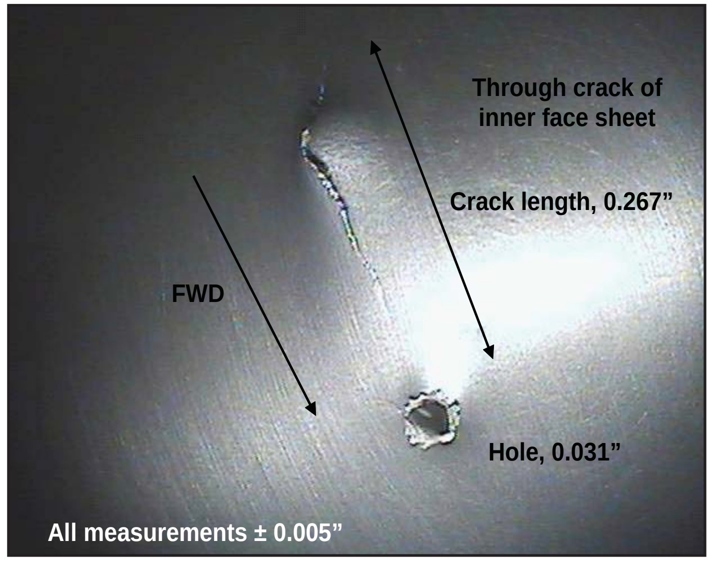

Figure 4. Rear facesheet damage on starboard radiator #4.

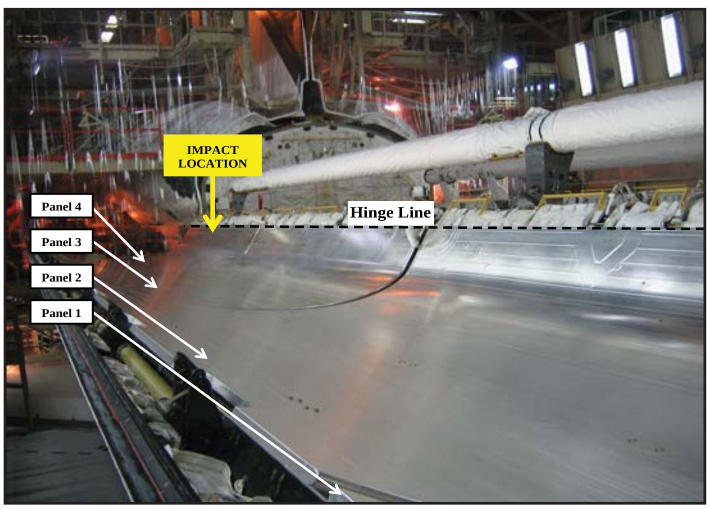

Figure 2. Orbiter payload bay door radiators (starboard panels 1-4 shown).

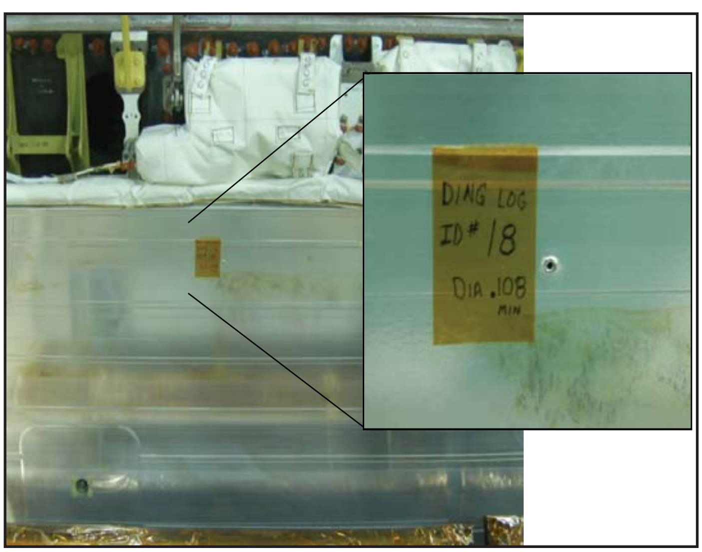

Figure 3. Front facesheet damage on starboard radiator #4.

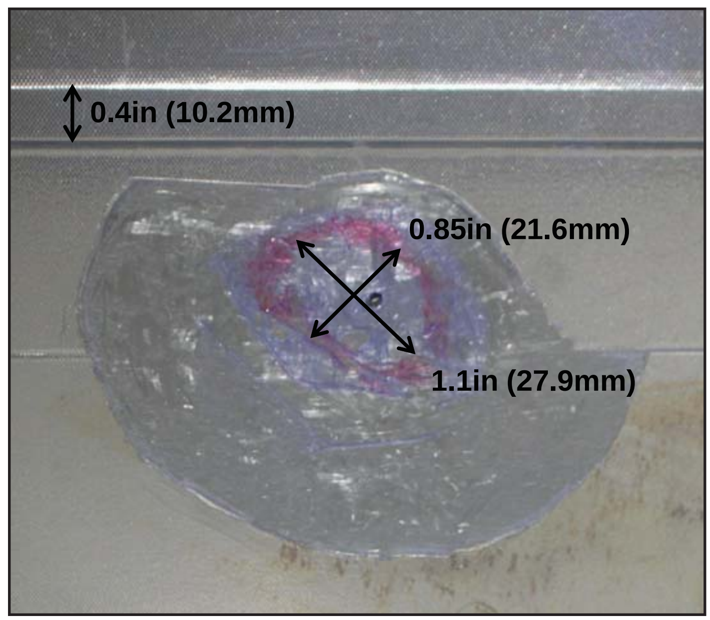

Figure 5. Front facesheet with thermal tape removed. Extent of damaged facesheet is hghlighted.

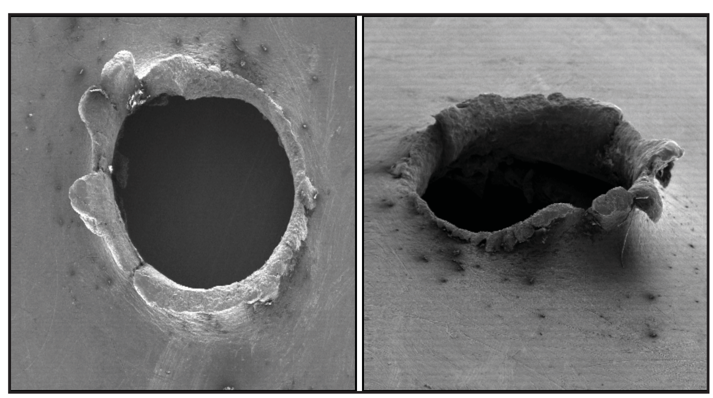

Figure 6. SEM images of hole in front facesheet. Asymmetric nature of lip can be seen in the oblique view.

MMOD Impact

continued from page 3

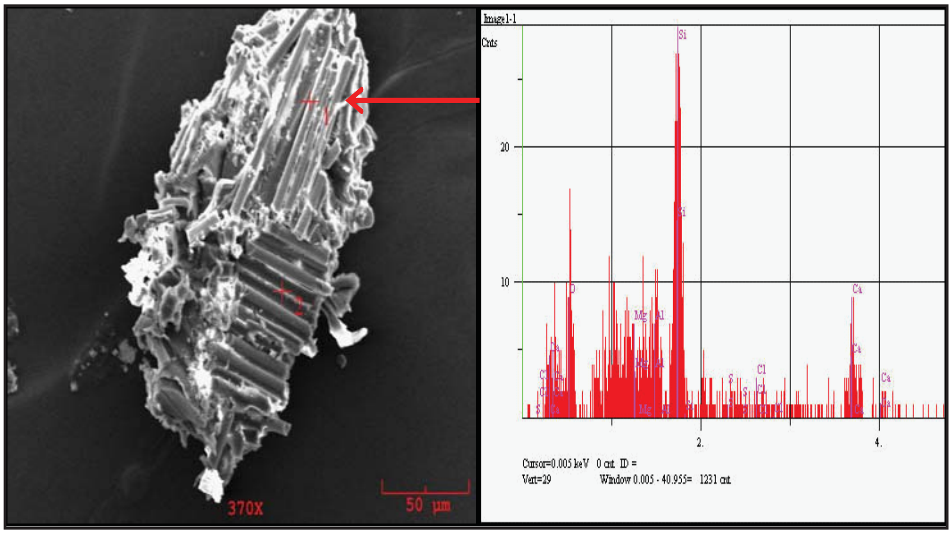

Figure 7. Example SEM image and EDS spectra of circuit board fragment.

height of the lip may be attributed to projectile shape and impact angle. Numerous instances of a glass-fiber organic matrix composite were observed in the facesheet tape sample. The fibers were approximately 10 micrometers in diameter and variable lengths. EDS analysis indicated a composition of Mg, Ca, Al, Si, and O. Figures 7 and 8 present images of the fiber bundles, which were believed to be circuit board material based on similarity in fiber diameter, orientation, consistency, and composition.

4. Hypervelocity Impact Tests

A test program was initiated in an attempt to simulate the observed damage to the radiator facesheet and honeycomb. Twelve test shots were performed using projectiles cut from a 1.6 mm thick fiberglass circuit board substrate

continued on page 5

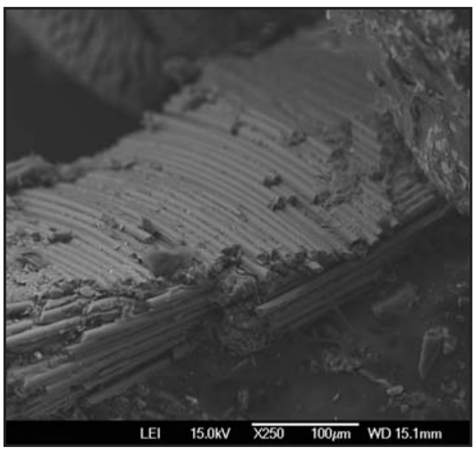

Figure 8. SEM image of circuit board fragment.

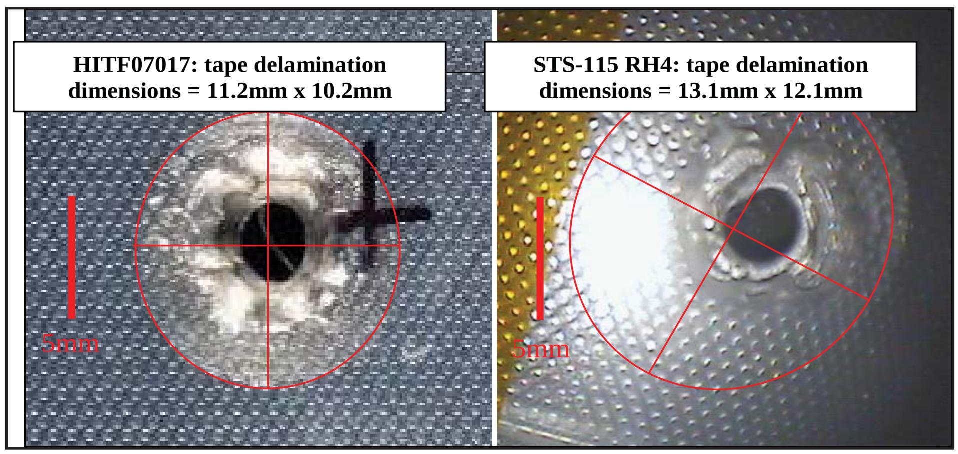

Figure 9. Entry hole in upper facesheet.

was found on thermal blankets or payload bay door structure under the radiator panel.

Figure 5 shows the front facesheet with the thermal tape removed. Ultrasound examination indicated a maximum facesheet debond extent of approximately 1 in. (25 mm) from the entry hole. X-ray examinations revealed damage to an estimated 31 honeycomb cells with an extent of 0.85 in. x 1.1 in. (21.6 x 27.9 mm).

3. SEM/EDS Analysis

Pieces of the radiator at and surrounding the impact site were recovered during the repair procedures at KSC. They included the thermal tape, front facesheet, honeycomb core, and rear facesheet. These articles were examined at JSC using a scanning electron microscope (SEM) with an energy dispersive x-ray spectrometer (EDS). Figure 6 shows SEM images of the entry hole in the facesheet. The asymmetric

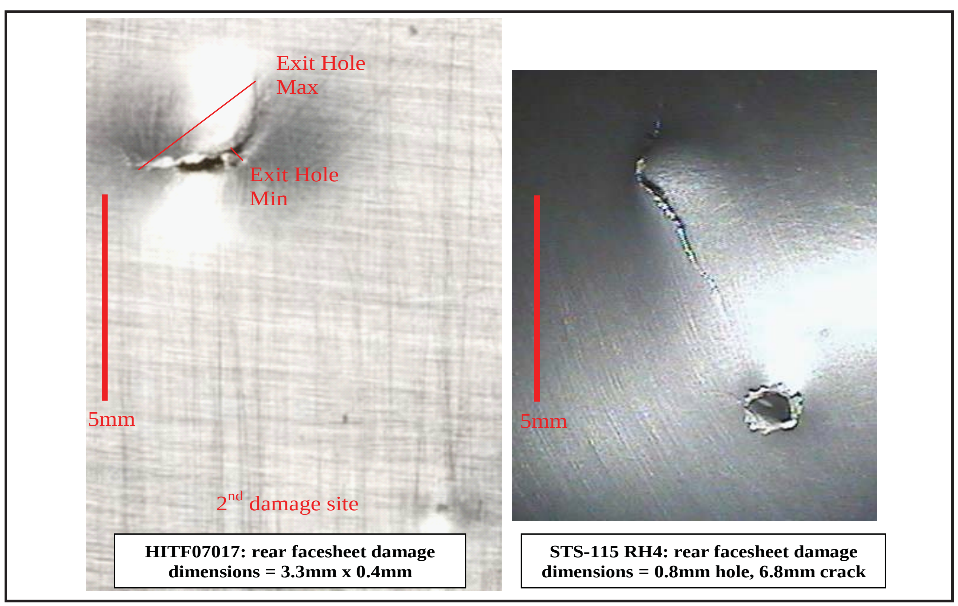

Figure 10. Exit hole in lower facesheet.

MMOD Impact

continued from page 4

panel. Results from test HITF07017, shown in figures 9 and 10, correlates with the observed impact features reasonably well. The test was performed at 4.14 km/sec with an impact angle of 45 degrees using a cylindrical projectile with a diameter and length of 1.25 mm. The fiberglass circuit board material had a density of 1.65 g/cm^3, giving a projectile mass of 2.53 mg.

5. Impact Risk

An analysis was performed using the Bumper code to estimate the probability of impact to the Shuttle from a 1.25 mm diameter particle. Table 1 shows a 1.6% chance (impact odds = 1 in 62) of a 1.25 mm or larger MMOD impact on the radiators of the vehicle during a typical ISS mission. There is a 0.4% chance (impact odds = 1 in 260) that a 1.25 mm or larger MMOD particle would impact the RCC wing leading edge and nose cap during a typical mission. Figure 11 illustrates the vulnerable areas of the wing leading edge reinforced carbon-carbon (RCC), an area of the vehicle that is very sensitive to impact damage. The highlighted red, orange, yellow, and light green areas would be expected to experience critical damage if impacted by an OD particle such as the one that hit the RH4 radiator panel on STS-115. ♦

Table 1. MMOD impact risk for a typical Shuttle mission to ISS from particles 1.25 mm and larger.

Region	MMOD Impact Risk	Odds of Impact
Upper TPS	7%	1 in 15
Lower TPS	1.7%	1 in 59
Radiators	1.6%	1 in 62
Wing Leading Edge and Nose Cap RCC	0.4%	1 in 260
Windows	0.04%	1 in 2500
Total Vehicle	10%	1 in 10

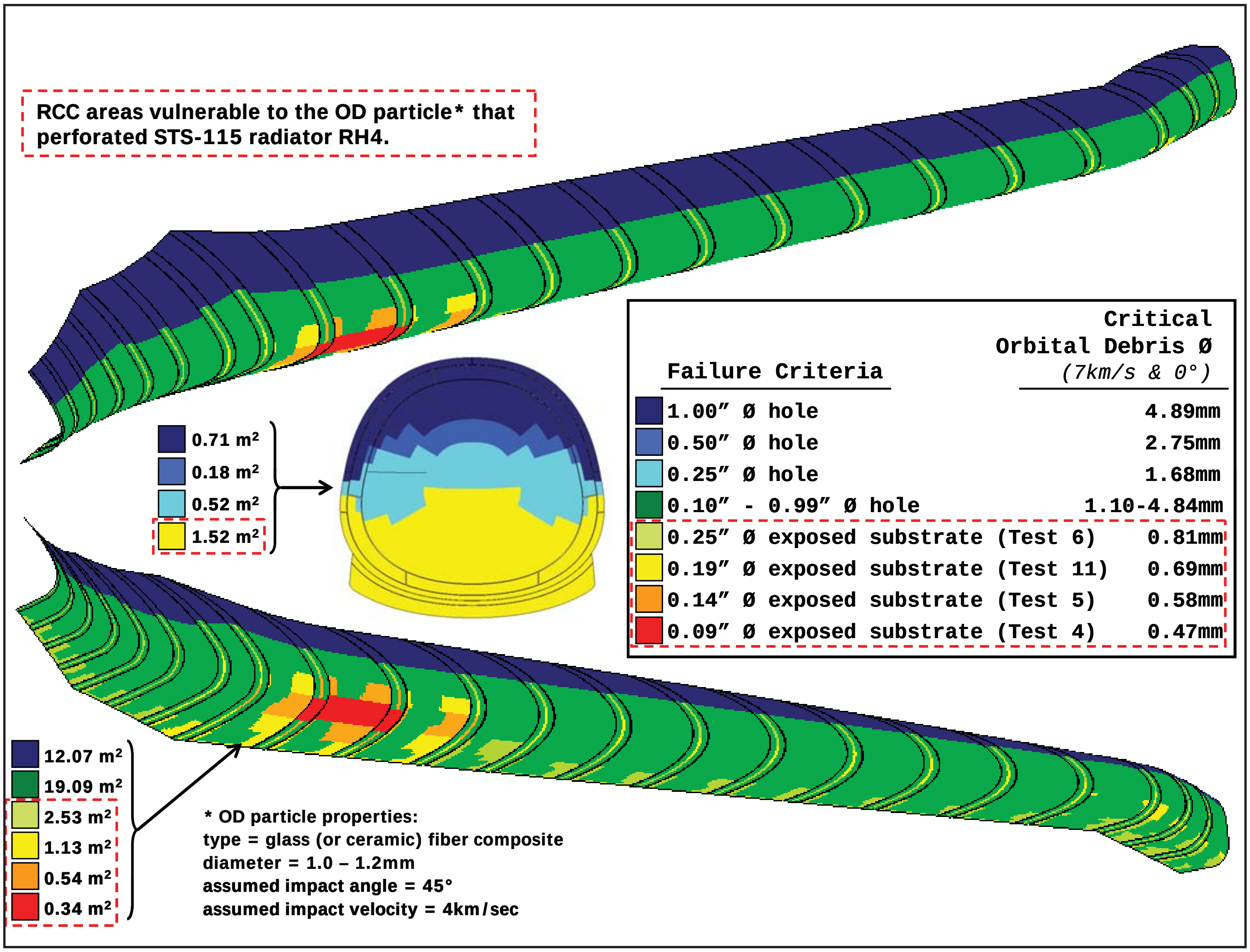

Figure 11. MMOD Failure Criteria for RCC: wing leading edge, nose cap and chin panel.

Optical Observations of GEO Debris with Two Telescopes

P. SEITZER, K. ABERCROMBY,
H. RODRIGUEZ, AND E. BARKER

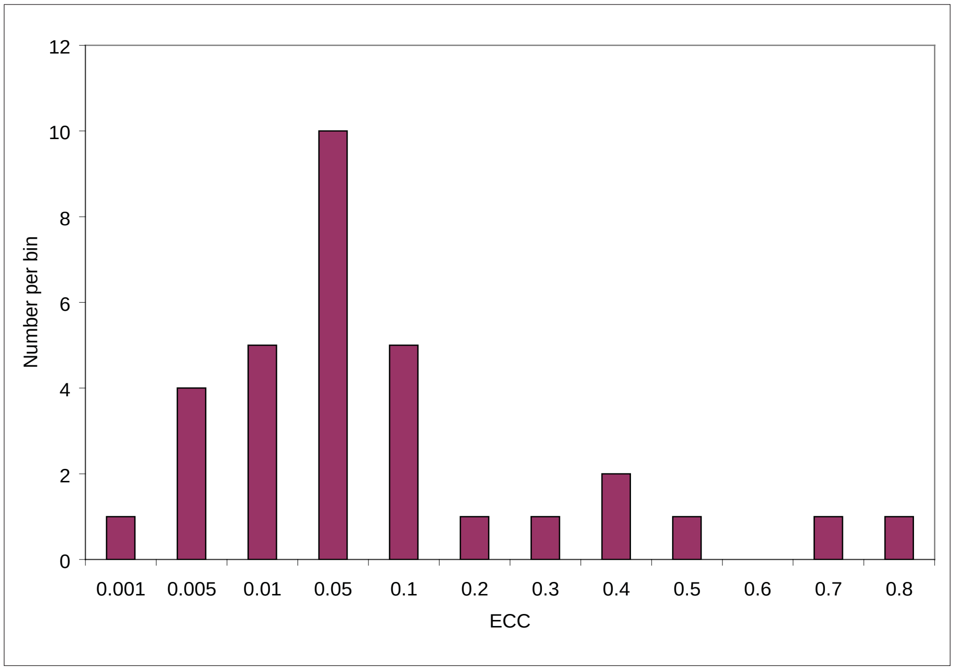

Figure 1. The eccentricity histogram of all objects (32) for which enough data exists to determine a full six-parameter orbit without the circular orbit assumption.

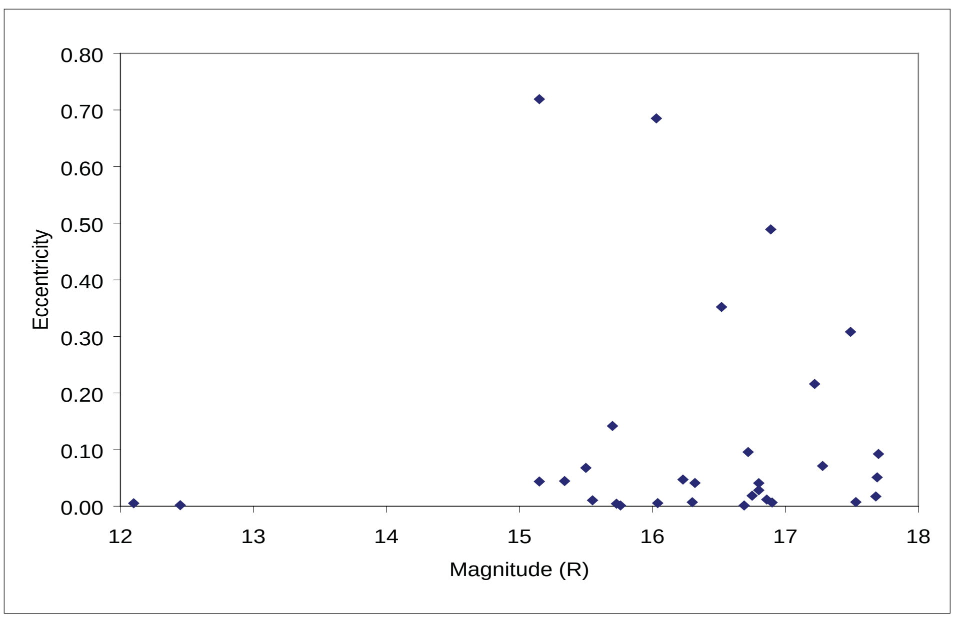

Figure 2. Eccentricity versus magnitude for each of the 32 objects for which a full six-parameter orbit was calculated.

For several years, the **M**ichigan **O**rbital **DE**bris **S**urvey **T**elescope (MODEST), the University of Michigan's 0.6/0.9-m Schmidt telescope on Cerro Tololo Inter-American Observatory in Chile, has been used to survey the debris population at GEO in the visible regime. Magnitudes, positions, and angular rates are determined for GEO objects as they move across the telescope's field-of-view (FOV) during a 5-minute window.

This short window of time is not long enough to determine a full six parameter orbit so usually a circular orbit is assumed. A longer arc of time is necessary to determine eccentricity and to look for changes in the orbit with time. MODEST can follow objects in real-time, but only at the price of stopping survey operations. A second telescope would allow for longer arcs of orbit to obtain the full six orbital parameters, as well as assess the changes over time. An additional benefit of having a second telescope is the capability of obtaining colors of the faint targets, aiding efforts to determine the material type of faint debris.

For 14 nights in March 2007, two telescopes were used simultaneously to observe the GEO debris field. MODEST was used exclusively in survey mode. As objects were detected, they were handed off in near real-time to the Cerro Tololo 0.9-m telescope for follow-up observations. The goal was to determine orbits and colors for all objects fainter than R = 15th magnitude (corresponds to 1 meter in size assuming a 0.2 albedo) detected by MODEST. The hand-off process was completely functional during the final eight nights and follow-ups for objects from night-to-night were possible.

The cutoff magnitude level of 15th was selected on the basis of an abrupt change in the observed angular rate distribution in the MODEST surveys. Objects brighter than 15th magnitude tend to lie on a well defined locus in the angular rate plane (and have orbits in the catalog), while fainter objects fill the plane almost uniformly. We need to determine full six-parameter orbits to investigate what causes this change in observed angular rates. Are these faint objects either the same population of high area-to-mass (A/m) objects on eccentric orbits as discovered by the ESA Space Debris Telescope (Schildknecht, et al., 2004), or are they just normal debris from breakups in GEO?

Our success rate in handing off was greater than 85%, despite the very small FOV of the 0.9-m telescope (only 0.22°, compared with 1.3° for MODEST). The average time from last detection on MODEST to first detection on the 0.9-m telescope was 17 minutes; the quickest was 4 minutes. Thus, the statistical completeness of the follow-up sample is very high.

Figure 1 shows a histogram of the 32 objects for which enough data was collected to determine the full orbit parameters. The majority of the objects were in circular orbits, but 20% of the objects had eccentricities greater than 0.2. Figure 2 depicts eccentricity versus magnitude and Figure 3 shows inclination versus right ascension of ascending node (RAAN) for the same set of objects.

The ability to run two telescopes simultaneously provides a very powerful probe

continued on page 7

Optical Observations

continued from page 6

of the GEO debris field. Initial observations indicate that we are seeing both circular and eccentric debris populations. We look forward to continuing these observations in the future. Our next run is planned for November 2007.

1. Schildknecht, *et al.*, *Properties of the High Area-to-mass Ratio Space Debris Population in GEO*, AMOS Technical Conference Proceedings, Kihei, Hawaii, pp. 216-224, September 2-5, 2005. ♦

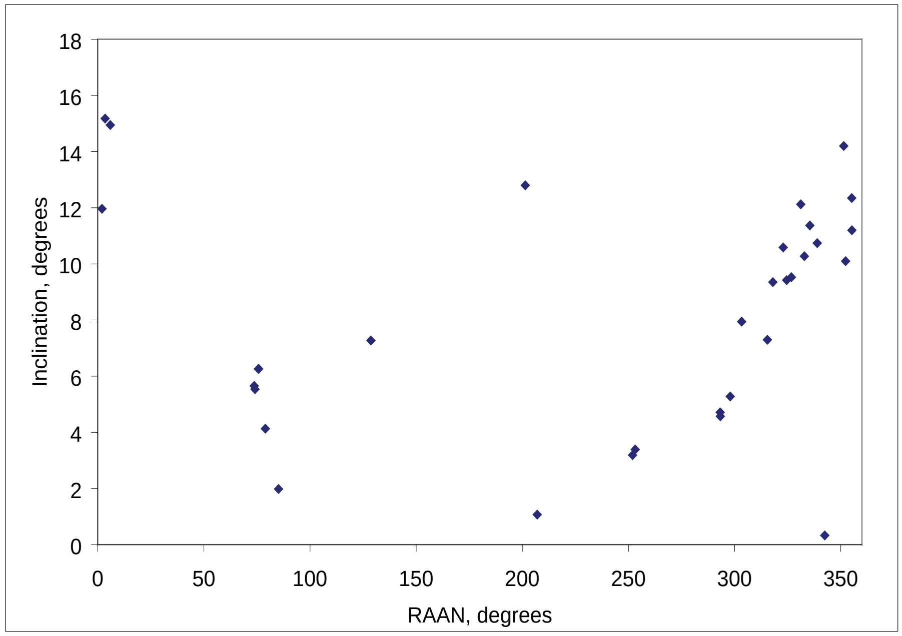

Figure 3. Inclination versus RAAN for each of the 32 objects in this specific dataset.

Optical Measurement Center Status

H. RODRIGUEZ, M. MULROONEY,
K. ABERCROMBY, AND E. BARKER

Beginning in 2005, an optical measurement center (OMC) was created to measure the photometric signatures of debris pieces. Initially, the OMC was equipped with a 300 W xenon arc lamp, a SBIG 512 x 512 ST8X MEI CCD camera with standard Johnson filters, and a Lynx 6 robotic arm with five degrees of freedom (Rodriguez et al., 2006) As research progressed, modifications were made to the equipment. A customized rotary table was built to overcome the robot's limitation of 180 degree wrist rotation and provide complete 360 degree rotation with little human interaction. This change allowed an initial phase angle (source-object-camera angle) of roughly 5 degrees to be adjusted to 7, 10, 15, 18, 20, 25, or 28 degrees. Additionally, the Johnson Red (R) and Infrared (I) CCD filters were replaced with the standard astronomical filters suite (Bessell R, I), keeping Johnson Blue (B) and Johnson Visible (V) filters. In an effort to reduce object saturation, the two generic aperture stops were replaced with neutral density filters.

Initially data were taken with aluminum debris pieces from the European Space Operations Centre ESOC2 ground test and more recently with samples from a thermal multi-layered insulation (MLI) commonly used on rocket bodies and satellites. The ESOC2 data provided light curve analysis for one type of material but many different shapes, including flat, bent, curled, folded, and torn (Rodriguez, et al., 2006). The MLI samples are roughly the same size and shape, but have different surfaces that give rise to interesting photometric light curves. In addition, filter photometry was conducted on the MLI pieces, a process that also will be used on the ESOC2 samples.

The MLI used for the current study consists of space-facing copper-colored Kapton with an aluminized backing for the top and bottom layers and alternating layers of DARCON or Nomex netting with aluminized Mylar for the middle layers. This material is significant to the study of space debris due to its high area-to-mass ratio (A/m) and the effect solar radiation pressure perturbations have on its orbital evolution. Measurements were taken at an 18 degree phase angle with one intact piece and three different layers of MLI, using the standard astronomical filters mentioned previously. The A/m ratios range from 2 to 10 m^2/kg. In Figure 1, a digital image of two pieces of MLI layering is displayed. The top left and right images are part of the outermost layer of MLI. The copper-colored Kapton is space-facing, while the silver color borders the interior MLI layers. The bottom left and right images are part of the spacecraft-facing MLI layer, with the copper-color Kapton facing the spacecraft while the silver color is positioned to the interior MLI layers.

Figure 1. Digital Images of sample MLI debris. Top images are part of the space-facing layer and the bottom images are part of the space-craft facing layer. The A/m for these samples is ~ 10 m^2/kg.

The following figure shows an example of intensity versus rotation over 360 degrees for the intact piece of MLI (see Figure 2). The pseudo-debris piece was rotated through five degree increments at a seven degree phase angle. Filter photometry data was taken through all five filters mentioned previously. The two intensity maxima around 90 and 270 degrees correspond to the maximum surface area of

continued on page 8

OMC Status

continued from page 7

the object facing the CCD camera. The object was rotated spacecraft side first, then space-facing side during the remaining 180 degrees of rotation. The structure in the light curve is due to the surface structure of the object — where the spacecraft facing layer is more uniform in composition, while the space-facing layer has a mesh structure on the edges and a perforated flat surface in the middle. If one were to compare the light curve of MLI to a flat plate rotated at the same phase angle over a 360 degree rotation, one would see that the flat plate would also show a bimodal plot of periodic motion with a set minimum and maximum.

In addition to photometric laboratory measurements, laboratory spectral measurements will be taken with the same MLI samples. Spectral data will be combined to match the wavelength region of photometric data so that a fiduciary reference can be established for the photometric measurements. Published spectral data of MLI shows a strong absorption feature near 4800 Angstroms, which is due to the copper color of Kapton (Jorgensen 2000). Space debris containing MLI may therefore be identified via telescopic observations employing either high resolution spectroscopy or narrow-band photometry. Furthermore, we will ascertain whether the absorption feature is sufficiently broad to enable identification via broad-band (R-B) photometry.

Using laboratory photometric and spectral measurements, an optical property database will be provided for an object with a high A/m made of similar materials to MLI. The benefits of this database for remote optical measurements of orbital debris will be shown by illustrating the optical properties expected for a high A/m object.

Future work will involve more complex rotations for different pieces of pseudo-debris and will incorporate other phase angles. An optical mirror is available for configuring the OMC for a 90 degree phase angle. The ongoing research is aimed towards developing an optical Size Estimation Model (SEM) comparable to the current radar SEM so that a better model may be obtained for the orbital space environment utilizing both radar and optical data.

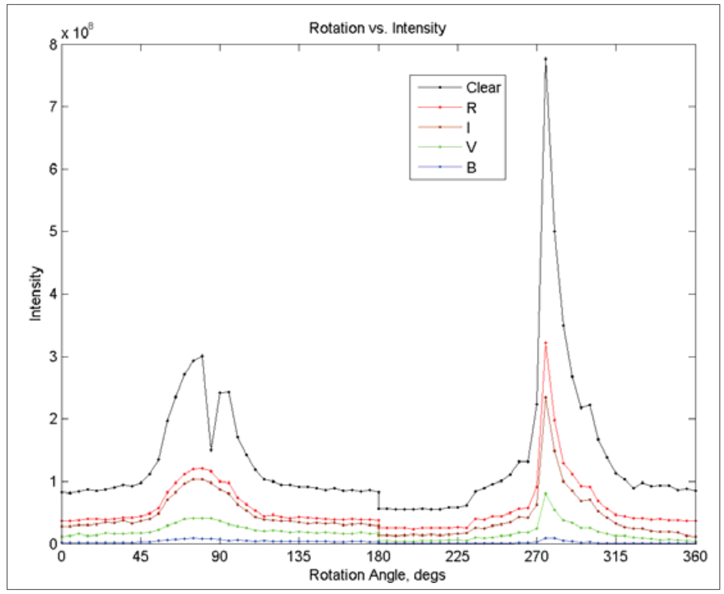

Figure 2. Intensity versus Rotation through five filters: Clear, Bessell R, Bessell I, Johnson B, and Johnson V.

1. Rodriguez, H.M., Abercromby, K. J., Jarvis, K. S., and Barker, E., *Orbital Debris Photometric Study,* ODQN, Vol. 10, Issue 2, 2006.

2. Rodriguez, H.M., Abercromby, K. J., Jarvis, K. S., and Barker, E., *Using Light Curves to Characterize Size and Shape of Pseudo-Debris,* 2006 AMOS Technical Conference, Maui, Hawaii, 10-14 September 2006.

3. Jorgensen, K., *Using Reflectance Spectroscopy to Determine Material Type of Orbital Debris*, Ph.D. Thesis, University of Colorado, Boulder, May 2000. ♦

ABSTRACTS FROM THE NASA ORBITAL DEBRIS PROGRAM OFFICE

Second International Association for the Advancement of Space Safety (IAASS) Conference 14-16 May 2007, Chicago, Illinois, USA

The Disposal of Spacecraft and Launch Vehicle Stages in Low Earth Orbit

N. JOHNSON

As a result of the increasing number of debris in low Earth orbit (LEO), numerous national and international orbital debris mitigation guidelines recommend the removal of spacecraft and launch vehicle stages from LEO within 25 years after mission termination. The primary purpose of this action is to enhance space safety by significantly limiting the potential of future accidental collisions resulting in the creation of large numbers of new orbital debris. Likewise, the passivation of these objects, i.e., the removal of residual stored energies, while they remain in orbit is important to prevent the generation of debris via self-induced explosions. Characteristics and trends in the growth of the derelict spacecraft and launch vehicle stage populations in LEO are examined.

Depending upon the final operational altitude of the vehicle, achieving the goal of orbital lifetime reduction can influence the design and deployment philosophy of a new space system. Some spacecraft and launch vehicle stages have combined their end-of-mission passivation operations with maneuvers to vacate long-lived orbital regimes. Perhaps

continued on page 9

The Disposal of Spacecraft

continued from page 8

the most dramatic demonstration of this type occurred in 2006 when a U.S. Delta IV second stage executed an unprecedented controlled-reentry maneuver from a circular orbit at an altitude near 850 km. For space systems in orbital regimes near the upper regions of LEO (i.e., between 1400 km and 2000 km altitude), maneuvers to place the vehicle above LEO might be more attractive than attempting to ensure an atmospheric reentry within 25 years, and at least one space system operator has selected this option. In some cases, careful consideration of natural orbital perturbations can also lead to reduced orbital lifetimes, although new launch constraints might need to be imposed.

The most important passivation measures for a spacecraft or launch vehicle stage are (1) the removal (normally by burning or venting) of residual propellants and pressurants and (2) the electrical discharge of batteries and, if applicable, their disconnection from charging circuits. Several examples of how a number of countries and international organizations have already been working to responsibly dispose of LEO spacecraft and launch vehicle stages are presented.

On the other hand, the adoption of such debris mitigation measures, although highly recommended, is not yet sufficiently practiced due to the design of the current generation of spacecraft and launch vehicles or due to other influences. Spacecraft with no maneuver capability and solid-propellant upper stages can pose serious challenges to compliance with disposal recommendations. As a class, small satellites, especially mini-, micro-, and pico-satellites, often fall short in their adherence to orbital debris mitigation guidelines. However, efforts are underway to identify cost-effective solutions. ♦

2007 Space Control Conference
1-3 May 2007, MIT Lincoln Laboratory, Lexington, Massachusetts, USA

GEO Population Estimates Using Optical Survey Data

E. BARKER, M. MATNEY

Optical survey data taken using the NASA Michigan Orbital DEbris Survey Telescope (MODEST) gives us an opportunity to statistically sample faint object population in the Geosynchronous (GEO) and near-GEO environment. This paper will summarize the MODEST survey work that has been conducted by NASA since 2002, and will outline the techniques employed to arrive at the current population estimates in the GEO environment for dim objects difficult to detect and track using current systems in the Space Surveillance Network (SSN).

Some types of orbits have a higher detection rate based on what parts of the GEO belt are being observed; a straightforward statistical technique is used to debias these observations to arrive at an estimate of the total population potentially visible to the telescope. The size and magnitude distributions of these fainter debris objects are markedly different from the catalogued population.

GEO debris consists of at least two different populations, one which follows the standard breakup power law and one which has anomalously high Area-to-Mass Ratios (1 to ~30 m^2/kg; a sheet of paper = ~13 m^2/kg).

The Inter-Agency Space Debris Coordination Committee (IADC) is investigating objects in GEO orbits with anomalously high Area-to-Mass Ratios (AMRs). The ESA Space Debris Telescope discovered this population and defined its general properties [inclinations (0 to 30 degrees), changing eccentricities (0 to 0.6), and mean motions (~1 rev)]. The accepted interpretation of this orbital behavior is that solar radiation pressure drives the perturbations causing time dependent inclinations and eccentricities. The orbital parameters are unstable for this population and thus difficult to predict. Their dim visual magnitudes and photometric variability make observations a challenge. The IADC has enlisted a series of observatories (participating institutions: University of Michigan/CTIO, Astronomical Institute University of Bern, Boeing LTS/AMOS, Keldysh Institute of Applied Mathematics) at different longitudes. Complete observational coverage over periods of days to months will provide a better understanding of the properties, such as solar radiation pressure effects on orbital elements, size, shape, attitude, color variations, and spectral characteristics.

Results from recent observational programs will be summarized, and includes a description of the orbit elements prediction processes, a summary of the metric tracking performance, and some photometric characteristics of this class of debris.

UPCOMING MEETINGS

12-15 September 2007: 2007 Advanced Maui Optical and Space (AMOS) Surveillance Technologies Conference, Wailea, Maui, Hawaii, USA.

The 2007 AMOS Conference will cover various topics in adaptive optics, astronomy, imaging, lasers, metrics, non-resolved object characterization, orbital debris, Pan-STARRS, Space Situational Analysis programs and systems, and telescopes and sensors. Additional information on the conference is available at http://www.amostech.com.

23-27 September 2007: Hypervelocity Impact Symposium (HVIS), Wiliamsburg, Virginia, USA.

This biennial symposium is dedicated to enabling and promoting an understanding of the basic physics of high velocity impact and related technical areas, including spacecraft shielding design and orbital debris environment. More information can be obtained at http://hvis.org/HVIS_07/index.html.

24-28 September 2007: The 58th International Astronautical Congress, Hyderabad, India.

A Space Debris Symposium is planned for the congress. The four scheduled sessions will address the complete spectrum of technical issues of space debris, including measurements and space surveillance, modeling, risk assessment, reentry, hyper-velocity impacts, protection, mitigation, and standards. Additional information is available at http://www.iac2007.org.

ORBITAL BOX SCORE

(as of 04 July 2007, as cataloged by US SPACE SURVEILLANCE NETWORK)

Country/ Organization	Payloads	Rocket Bodies & Debris	Total
CHINA	62	2234	2296
CIS	1362	2919	4281
ESA	37	36	73
FRANCE	45	316	361
INDIA	33	106	139
JAPAN	101	73	174
US	1069	3120	4189
OTHER	386	55	441
TOTAL	3095	8859	11954

Technical Editor
J.-C. Liou

Managing Editor
Debi Shoots

Correspondence concerning the ODQN can be sent to:
Debi Shoots
NASA Johnson Space Center
Orbital Debris Program Office
Mail Code JE104
Houston, TX 77058

debra.d.shoots@nasa.gov

MEETING REPORT

The second conference of the recently established International Association for the Advancement of Space Safety (IAASS) was held in Chicago during 14-16 May. Sessions on orbital debris hazards and reentry risks spanned a day and a half of the conference, including topics on the disposal of spacecraft and rocket bodies in low Earth orbit, nuclear reactor coolant droplets in long-lived orbits, protection of space vehicles from micrometeoroid and orbital debris particles, and reaction wheel designs to minimize reentry risks. A new committee on space debris is being formed under the IAASS. The next conference of the IAASS will be held in Rome during 21-23 October 2008. ♦

National Aeronautics and Space Administration

Lyndon B. Johnson Space Center
2101 NASA Parkway
Houston, TX 77058

www.nasa.gov

INTERNATIONAL SPACE MISSIONS

29 March - 30 June 2007

International Designator	Payloads	Country/ Organization	Perigee (KM)	Apogee (KM)	Inclination (DEG)	Earth Orbital Rocket Bodies	Other Cataloged Debris
2007-008A	SOYUZ-TMA 10	RUSSIA	329	340	51.6	1	0
2007-009A	ANIK F3	CANADA	35777	35796	0.0	1	1
2007-010A	HAI YANG 1B	CHINA	783	814	98.6	1	0
2007-011A	BEIDOU M1	CHINA	21518	21545	55.3	1	0
2007-012A	EGYPTSAT 1	EGYPT	657	666	98.1	1	1
2007-012B	SAUDISAT 3	SAUDI ARABIA	657	678	98.1		
2007-012C	SAUDICOMSAT 7	SAUDI ARABIA	652	739	98.1		
2007-012E	SAUDICOMSAT 6	SAUDI ARABIA	649	761	98.1		
2007-012F	AEROCUBE 2	USA	649	769	98.1		
2007-012H	SAUDICOMSAT 5	SAUDI ARABIA	653	728	98.1		
2007-012J	SAUDICOMSAT 3	SAUDI ARABIA	654	717	98.1		
2007-012K	MAST	USA	648	782	98.1		
2007-012L	SAUDICOMSAT 4	SAUDI ARABIA	650	750	98.1		
2007-012M	CP3	USA	647	792	98.1		
2007-012N	LIBERTAD 1	COLOMBIA	647	792	98.1		
2007-012P	CAPE 1	USA	647	792	98.1		
2007-012Q	CP4	USA	649	770	98.1		
2007-012R	CSTB 1	USA	649	770	98.1		
2007-013A	AGILE	ITALY	523	552	2.5	1	0
2007-014A	NFIRE	USA	489	497	48.2	1	0
2007-015A	AIM	USA	584	602	97.8	1	0
2007-016A	ASTRA 1L	LUXEMBOURG	35725	35727	0.1	1	1
2007-016B	GALAXY 17	INTELSAT	35729	35785	0.0		
2007-017A	PROGRESS-M 60	RUSSIA	329	340	51.6	1	0
2007-018A	NIGCOMSAT 1	NIGERIA	35784	35788	0.1	1	0
2007-019A	YAOGAN 2	CHINA	630	656	97.9	0	0
2007-020A	GLOBALSTAR	USA	914	932	52.0	1	1
2007-020C	GLOBALSTAR	USA	831	864	52.0		
2007-020D	GLOBALSTAR	USA	1413	1414	52.0		
2007-020F	GLOBALSTAR	USA	919	937	52.0		
2007-021A	SINOSAT 3	CHINA	35784	35792	0.2	1	0
2007-022A	COSMOS 2427	RUSSIA	180	335	67.1	1	1
2007-023A	COSMO-SKYMED 1	ITALY	621	624	97.9	1	0
2007-024A	STS 117	USA	334	354	51.6	0	0
2007-025A	OFEQ 7	ISRAEL	343	576	141.8	1	0
2007-026A	TERRA SAR X	GERMANY	507	510	97.4	1	1
2007-027A	USA 194	USA	NO ELEMS. AVAILABLE			1	1
2007-028A	GENESIS 2	USA	556	562	64.5	1	1
2007-029A	COSMOS 2428	RUSSIA	846	857	71.0	1	4